Computational study of electron states in Au chains on NiAl(110)

Mats Persson*

Department of Applied Physics, Chalmers/Göteborgs University, S-41296, Göteborg, Sweden
(Received 31 May 2004; published 18 November 2004)

We have carried out a density functional study of unoccupied, resonance states in a single Au atom, dimers, a trimer, and infinite Au chains on the NiAl(110) surface. Two inequivalent orientations of the ad-chains with substantially different interatomic distances were considered. From the study of the evolution of the electron states in an Au chain from being isolated to adsorbed, we find that the resonance states derive from the $6s$ states of the Au atoms, which hybridize strongly with the substrate states and develop a p-like polarization. The calculated resonance states and the local density of states (LDOS) images were analyzed in a simple tight-binding, resonance model. This model clarifies (1) the physics of direct and substrate-mediated adatom-adatom interactions and (2) the physics behind the enhancements of the LDOS at the ends of the adatom chains, and (3) the physical meaning of the "particle-in-box" model used in the analysis of observed resonance states. The calculated effective mass and band bottom energy are in good agreement with experimental data obtained from scanning tunnelling spectroscopy.

I. INTRODUCTION

A most interesting development in nanoscience has been the possibility to tailor and analyze the electronic properties of single nanostructures of adatoms on metal surfaces, This development has been made possible by the unique capabilities of the scanning tunnelling microscope (STM) to image and manipulate single adatoms and to probe their electronic structure by tunnelling spectroscopy. A pioneering example is provided by the quantum corral experiments, in which atomic manipulations were used to assemble closed atomic structures, which in turn act as two-dimensional resonance cavities for surface state electrons on a metal surface.[1,2] Another most interesting example is provided by the unoccupied, electron resonance states in Au adatom and addimers[3] and longer Au ad-chains[4–7] assembled on a NiAl(110) surface, which were revealed by imaging the differential conductance for various biases. This class of resonance states was also identified in linear Cu chains on Cu(111) (Ref. 8) so their existence is not limited to the NiAl(110) substrate.

The appearance of such resonance states in Au adatom structures was rather surprising and raises several questions about their physical nature. In the original experiments,[4,5] the differential conductance spectra and images of linear Au ad-chains were analyzed using the quantum states of a simple, one-dimensional "particle-in-box" (PIB) model. The observed dispersion of the resonance states in the Au chain was found to be free-electron-like with an effective mass being about one-half of the bare mass and the observed dependence of the low energy peak position on the ad-chain length followed closely the prediction of the PIB model. However, the origin and the character of these resonance states were not clarified in this model and the physical meaning of the one-dimensional "box" is unclear in view of the discrete atomic structure of the ad-chains. Thus there is a need to gain a more detailed understanding of these resonance states from calculations and modelling of their electronic structure.

The unoccupied, resonance states of the Au adatom structures are excited states that are probed by adding an extra electron. In principle, they are not directly described by a conventional density functional theory. However, unoccupied, Kohn-Sham states provide a useful, zero-order approximation of such excited states[9] as demonstrated by density functional calculations of a single Au adatom and ad-dimers with various interatomic separations. These calculations showed that the observed resonance structures in the scanning tunneling spectra (STS) were reproduced in the calculated local density of states (LDOS) at the tip apex.[3] These resonances were formed in an energy region with a depletion of LDOS and had a mixed s and p character.

A first attempt to understand the nature of the resonance states of the Au ad-chains was the recent density functional study of isolated, finite Au chains by Mills and co-workers.[10] They argued that the observed resonance states derived from unoccupied states with π character of the isolated chains. This argument resolved the issue that the observed lowest energy state with no nodes along the chain is unoccupied in contrast to the states of the isolated chains with σ character. Furthermore, they introduced a three-dimensional "particle-in-a-cylinder" model to rationalize all STM observations. However, this study did not address the effects of the interaction of the states in the Au chains with the substrate states.

In this paper, we present a density functional study of the resonance states of some linear Au adatom structures adsorbed along two inequivalent directions on the NiAl(110) surface. The focus is primarily on the infinite Au ad-chains of which one has the same orientation along the [001] direction as an assembled chain,[4,5] whereas the other infinite, Au ad-chain is oriented along the $[1\bar{1}0]$ direction. The substantially larger interatomic distance of the latter ad-chain than the former ad-chain illustrates the effects of interatomic interactions on the electronic states. We present also results for a single adatom, two different ad-dimers and an ad-trimer. The nature of the resonance states in the infinite ad-chains is revealed by studying their evolution from the states of the infinite, isolated Au chains with decreasing chain-surface distance. We also discuss the calculated resonance states and

the tunnelling through the resonance states in terms of a tight-binding, resonance model. This model clarifies the physical meaning of the "particle-in-box" model in the analysis of the resonance states.

The paper is organized in the following manner. In Sec. II, we present some details of the density functional calculations of the adatom structures and their geometric and electronic structure are presented in Sec. III. The nature of the resonance states in the Au ad-chains and their relation to the states of the isolated Au chains are discussed in Sec. IV A. A simple, tight-binding resonance model for the states in the adatom structures is described in the Appendix and discussed in relation to calculated resonance energies and images in Sec. IV B. Our results are compared with experimental data in Sec. V, where we also clarify the physical meaning of the "particle-in-box" model in terms of the tight-binding, resonance model. Finally, we give some concluding remarks in Sec. VI.

II. COMPUTATIONAL METHOD

We have considered several linear Au adatom structures on the NiAl(110) surface including single adatoms, two different ad-dimers and infinite, ad-chains along either the [001] direction or the $[1\bar{1}0]$ direction and an ad-trimer along the [001] direction. The [001] and the $[1\bar{1}0]$ directions correspond to the $\bar{\Gamma}$-$\bar{Y}$ and the $\bar{\Gamma}$-$\bar{X}$ directions in the surface Brillouin zone (SBZ), respectively,[11] so that the corresponding chains aligned along these two directions are henceforth referred to as the Y and X chain, respectively. The density functional calculations of the single adatoms and the two ad-dimers have already been briefly described in Ref. 3.

The electronic and the geometric structure of the Au chains and the trimer on NiAl(110) were studied using density functional calculations that were carried out using the projector augmented wave method as implemented in the VASP code.[12–14] The exchange and correlation effects were represented by the widely used PW91 version[15] of the generalized gradient approximation. The various versions of the GGA give similar results for atomic chemisorption and their limitations and differences are more significant in molecular chemisorption.[16,17] The two infinite (periodic) chain structures were represented by an Au adatom on a NiAl slab in two different supercell geometries. To minimize the interactions between the chain and its periodic images, we used a 1×4 and 6×1 surface unit cells for the Y and X chains, respectively. The results for the electronic states of the Y chain were found to be well converged for nine substrate layers and this number of layers was also used for the X chain. The vacuum region of the supercell was six layers. For the adtrimer we used a supercell with a 5×2 surface unit cell and eight layers of NiAl. The kinetic energy cutoff for the plane wave basis set was about 200 eV and the surface Brillouin zone was sampled by 80, 28, and 24 k points for the Y, X ad-chains, and the ad-trimer, respectively. The Au atom and the two outermost layers of Ni and Al atoms were fully relaxed until the residual forces were less than 0.05 eV/Å.

To make contact with scanning tunnelling spectra, we have calculated the local density of states outside the surface.

This approach is based on the Tersoff-Hamann (TH) approximation for tunnelling in an STM junction.[18] In this approximation, the differential conductance, $(dI/dV)(V)$, as defined from the tunnelling current I as a function of sample bias V, is given by

$$\frac{dI}{dV}(V = (\epsilon - \epsilon_F)/e) \propto \rho(\vec{r}_0, \epsilon) \qquad (1)$$

$$= \sum_{\mu} |\psi_{\mu}(\vec{r}_0)|^2 \delta(\epsilon - \epsilon_{\mu}). \qquad (2)$$

Here the local density of states, $\rho(\vec{r}_0, \epsilon)$, at the position $\vec{r}_0$ of the tip apex is expanded in wave functions $\psi_{\mu}(\vec{r}_0)$ of Kohn-Sham states μ with energy ϵ_{μ} of the sample in the absence of the tip and ϵ_F is the Fermi energy. The continuum of one-electron states is mimicked in the slab calculations by a Gaussian broadening of the delta function in Eq. (2). In principle, the range of applicability for TH approximation to the differential conductance is limited to small V. At larger V, one must in principle take into account both the change of the electronic states by the electric field from the tip and the V dependence of the tunnelling barrier. As suggested by Lang,[19] we have accounted for the latter effect by extending the wave functions into the vacuum region using a decay parameter set by the V-dependent vacuum barrier half-way from the surface to the tip apex.

III. RESULTS

In this section we will present our results for the LDOS of the various adatom structures in the progression of adatoms, ad-dimers, linear ad-trimers to infinite chains of Au atoms on the NiAl(110) surface. The effects of the adatom-adatom distance on the resonance states are revealed by considering the alignment of the ad-dimer and the ad-chain along the two inequivalent X and Y directions of the NiAl(110) surface as defined in Sec. II.

We begin by presenting the results for the geometries of the various linear adatom structures studied in this work. Following the suggestion by the STM experiments, we started our structural optimization by placing the Au adatoms in the short Ni bridge sites. In the optimization for the ad-dimers and the ad-trimer, we find that the adatom-adatom interactions are weak compared to the adatom-substrate interactions so that all adatoms are located laterally within 0.03 Å from the short Ni bridge positions. Thus the adatom-adatom distance is about 2.9 Å and 4.1 Å for the linear, adatom structures along the Y and the X directions, respectively. However, the structures with the short adatom-adatom distance tend to increase slightly the adatom-surface distance and relax slightly some surface Ni atom positions. The adatom-surface distance increases from 1.95 Å for the single adatom to 2.05 Å for the ad-chain along the Y direction. The bare NiAl(110) surface was found to be rumpled with the Al rows being displaced 0.18 Å farther out from the surface than the Ni rows in good agreement with earlier experimental and theoretical studies.[11,20] The only substantial adatom-induced substrate relaxation was found for the linear struc-
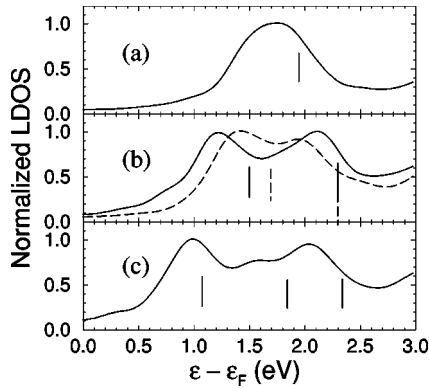
FIG. 1. Local density of states (LDOS) of (a) a single Au adatom and (b) Au ad-dimers on NiAl(110), and (c) Au ad-trimer. (b) Solid and dashed lines is the LDOS for the ad-dimer along the Y and X directions, respectively. The LDOS corresponds to a tip-surface distance of about 7 Å and in a position either (a) on top of the adatom, (b) laterally displaced 1 Å away from an adatom along the dimer axis, or (c) on top of an edge adatom. The measured peak energies as taken from Refs. 3 and 7 are also indicated by vertical bars.

tures along the Y direction and involved a downward relaxation by about 0.1 Å of the Ni atoms that are coordinated to two Au adatoms.

The results for the LDOS of the bare NiAl(110) surface, the single adatom and the two ad-dimers are shown in Fig. 1. As already reported and discussed in Ref. 3, the LDOS of the single Au adatom exhibits a single resonance peak in the unoccupied LDOS at about 1.71 eV, which is split into a resonance doublet in the LDOS for the two ad-dimers. The result for the LDOS of the clean surface showed a depletion in the structureless LDOS in this energy range and exhibited a sharp onset around 2.5 eV above the Fermi energy. The physical origin of these resonance states will be discussed further in Sec. IV A. From the character of the LDOS images at the peak energies, the low-lying state in the resonance doublet of the ad-dimer was shown to be a symmetric combination and an antisymmetric combination of the resonance states of the single adatoms in accordance with a simple, two-state model. The larger resonance splitting for the ad-dimer along the Y direction than along the X direction is simply caused by the stronger adatom-adatom interaction for the shorter ad-dimer than for the longer ad-dimer.

In the case of the linear ad-trimer, the interactions among the three adatom resonances give rise to a resonance triplet, as shown in Fig. 1(c). The maximum resonance energy splitting is about 1.0 eV and is larger than the energy splitting of 0.9 eV for the Y ad-dimer. The characters of the resonance states are also revealed by LDOS images at the resonance peak energies, as shown in Fig. 2. Note that the image for the lowest-lying resonance state has no nodal planes, whereas the other states have an increasing number of nodal planes with increasing resonance energy. The resonance energy positions and characters of these states and the strong intensity of the end lobes in the LDOS image of the highest lying resonance state will be discussed in Sec. IV B.

In the case of longer ad-chains, the interactions among the increasing number of adatom resonance states should even-
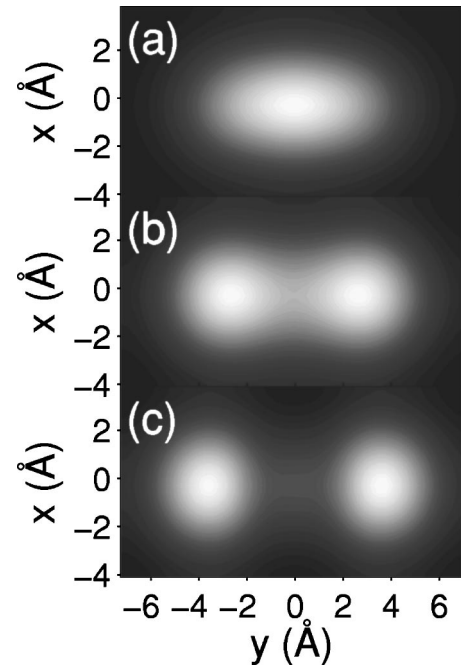
FIG. 2. Local density of states images of resonance states for the Au trimer on NiAl(110). (a) First state at 1.0 eV, (b) second state at 1.6 eV, and (c) third state at 2.0 eV. The origin is located at the center atom of the ad-trimer. Same tip-surface distance as in Fig. 1.

tually give rise to a band of resonance states for the infinite ad-chains. The formation of such a band is shown in the LDOS in Fig. 3 for the infinite ad-chains along the Y and X directions. The stronger adatom-adatom interactions for the Y ad-chain than for the X ad-chain results in a larger bandwidth for the Y ad-chain than for the X ad-chain. The dispersions of the bands of resonance states are revealed by the resolution of the LDOS over wave vectors in the one-dimensional Brilluion zones (LBZ) of the two ad-chains. In Fig. 4, we show contour plots of these wave-vector-resolved LDOS. These results show that the LDOS exhibit a resonance structure that disperses with the wave vector up to the middle of LBZ where the dispersion levels off and the resonance becomes ill-defined. For small wave vectors the dispersion is free-electron-like with an effective mass of 0.65 and 0.91 m_e for the Y and X ad-chains, respectively.
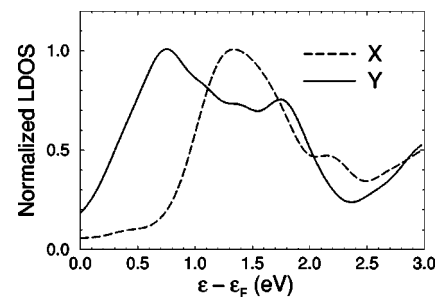
FIG. 3. Local density of states of the Au chains on NiAl(110) along the (a) Y and (b) X directions. The tip is above an Au atom at the same distance as in Fig. 1.
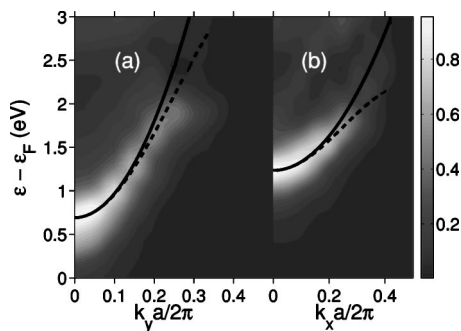
FIG. 4. Wave-vector-resolved local density of states of the Au chains on NiAl(110) along the (a) Y and (b) X directions. The dashed lines are dispersions as obtained from a nearest neighboring tight binding model, whereas the solid lines are the corresponding free particle dispersions with the same effective mass.

IV. DISCUSSION

In this section we will discuss the physical origin of the resonance states in the Au adatom structures on NiAl(110). This discussion concerns primarily the formation of the resonance states in the one-dimensional Au ad-chains. The energy positions and the LDOS images of the resonance states of the adatom structures will be discussed in a simple, tight-binding, resonance model. This model enables us also to discuss the LDOS images of ad-chains with arbitrary lengths.

A. Nature of the resonance states in the Au ad-chains

The existence of resonance states in Au adatom structures on the NiAl(110) surfaces raises several questions concerning the relation of these states to the states of the isolated adatom structures and the role played by the electronic states of the substrate. These questions are addressed here by scrutinizing the resonance states of the infinite ad-chains. We begin by discussing the states of the isolated Au chains.

In Figs. 5(a) and 5(b), we show the calculated band structures for the isolated Au chains with the same geometry as the ad-chains along the Y and X directions. These results are easily understood in terms of the electronic structure of an isolated Au atom as obtained from spin-unpolarized density
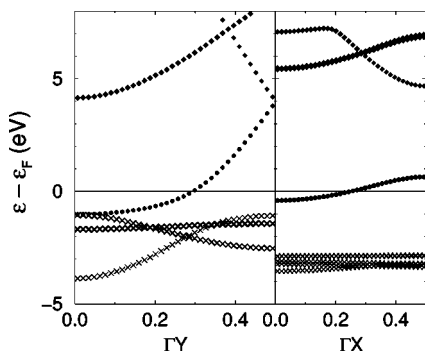
FIG. 5. Band structure of the isolated Au chains with same interatomic distances as the ad-chains along the (a) Y and (b) X directions. Bands with predominantly s, p, and d character are marked by solid circles, diamonds, and crosses, respectively.
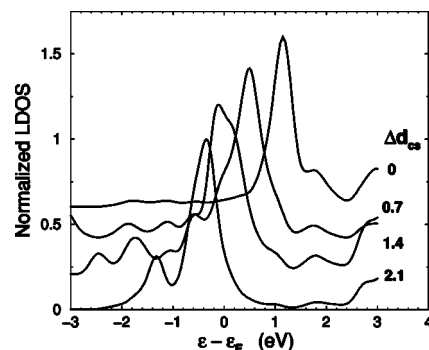
FIG. 6. Evolution of local density of states of the infinite, Au chain on NiAl(110) along the Y direction with outward displacement Δd_{cs} of the ad-chain from its equilibrium distance. The tip-ad-chain distance is kept at a fixed distance of 3 Å above an Au atom.

functional calculations. The fivefold, spatially degenerate $5d$ states of an Au atom are fully occupied with an energy 1.8 eV below the energy of the singly occupied $6s$ state. The threefold, spatially degenerate $6p$ states are unoccupied and located about 5 eV above the $6s$ state. When forming an infinite chain these atomic states overlap and form bands. In the case of the X chain, the interatomic distance is about 4.1 Å and the atomic states form narrow and nonoverlapping bands with predominantly atomic character as shown in Fig. 5(b). Only the $6p$ states show an appreciable bandwidth because they are close in energy to the vacuum level so that the corresponding wave functions are extended and have a large overlap. For the Y chain with a shorter interatomic distance of about 2.9 Å, the dispersion of the $5d$ and $6s$ states increase substantially compared to the X chain and develop a mixed character. The behavior of these band structures does not provide a simple answer to the question which atomic states are involved in the formation of the unoccupied resonance states in the ad-chain. The $6p$ bands are unoccupied but are far away from the Fermi level and the $6s$ band is half-occupied.

To understand how the resonance states of the Au ad-chains are related to the states of the isolated Au chains, we have calculated the evolution of the LDOS and the partial DOS for an Au atom in the Y ad-chain at the Γ point of the LBZ as a function of the outward rigid displacement Δd_{cs} of the chain from its equilibrium position. In Fig. 6, we show the calculated LDOS at a fixed distance of 3 Å outside the chain as a function of Δd_{cs}. At the largest Δd_{cs} of 2.1 Å, the chain-substrate coupling is weak and the LDOS have a prominent peak that is close in energy to the occupied states of s character of the isolated chain. For decreasing d_{cs}, this state of dominant s character of the chain shifts upward in energy and broadens into the unoccupied resonance state at the equilibrium position of the chain. Thus there is no indication in these results for the LDOS that this resonance state evolves from a $6p_z$ state of the Au chain that is broaden into a resonance and shifted down continuously in energy with decreasing Δd_{cs}. However, the result that the occupied $6s$ state of the chain at the Γ point turns into a narrow unoccupied resonance upon adsorption appears to indicate that the ad-chain is not charge neutral. This conflicting result is re-
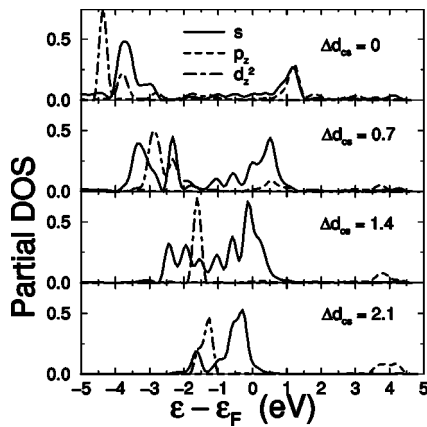
FIG. 7. Partial wave decomposition of the density of states for an Au atom in the chain on NiAl(110) along the Y direction for different outward displacements, Δd_{cs}, of the ad-chain from its equilibrium ad-chain-surface distance, as indicated in the figure.

solved by scrutinizing the evolution of the partial DOS.

In Fig. 7, we show the evolution of the partial DOS for an Au atom with s, p_z, and d_{z^2} characters at the Γ point in the chain BZ as a function of Δd_{cs}. At the largest Δd_{cs} of 2.1 Å, the chain is essentially decoupled from the substrate and the partial DOS exhibit peaks at energies close to the energies of the states of the isolated Au chain. The state at about 0.5 eV below the Fermi level has s character and broadens appreciably with decreasing Δd_{cs} and develops both a resonance structure in the unoccupied states and resonance structures in the occupied states well below the Fermi level. Thus the formation of both occupied and unoccupied states shows that the formation of the resonance with s character in the unoccupied states is not in conflict of the ad-chain being neutral. The partial DOS shows also that the resonance state has a strong p_z character at the equilibrium position but no significant d_{z^2} character. The development of the p_z character of the resonance state with decreasing Δd_{cs} is not correlated with the $6p_z$ state of the isolated, chain but involves rather a polarization. This latter state broadens substantially into a wide band upon adsorption with decreasing Δd_{cs} and does not shift continuously down in energy.

The calculated band structure of the bare NiAl(110) surface shows that there are projected band gaps in a energy region where the resonance state of the ad-chain X at the Γ point is formed. In Fig. 8, we show the calculated electronic states of a slab with 18 substrate layers along the Γ-X and Γ-Y directions in the surface BZ (SBZ) of NiAl(110). Only states that are even with respect to the symmetry planes spanned by these directions in the SBZ and the surface normal are shown in Fig. 8. The Γ point in the LBZ of the ad-chain X corresponds to the line of k points along the Γ-X direction in the SBZ. Along this line there is a projected band gap in an energy region that embraces the resonance energy about half-way to the LBZ boundary which shows that this resonance state is indeed a resonance since it overlaps with the bulk states.

A depletion of density of states in the energy region of the Au adatom-induced resonance states is revealed in the bulk DOS. In Fig. 9, we compare the calculated DOS for bulk
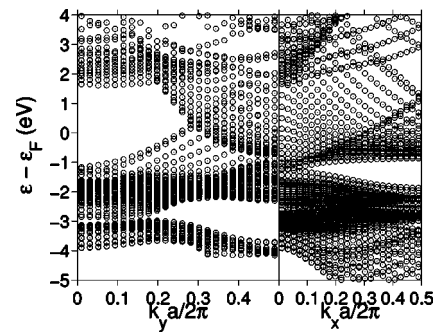
FIG. 8. Projected band structure of the isolated NiAl(110) surface as a function of the reduced wave vector along the Y and X directions. Only states with even character with respect to these directions have been displayed. The bands were calculated for an 18 layer slab.

NiAl and Cu. In the energy range of about -5 to -2 eV the DOS is dominated by the d states. In the case of NiAl, the transition metal atoms are surrounded by a simple metal atom resulting in a much narrower d band than for Cu. At larger energies the DOS are dominated by states with sp character. In the case of NiAl there is a depletion in the DOS in energy range from about 0 to 2.5 eV, whereas Cu shows no such depletion of the DOS. Note that this depletion is not a necessary condition for the formation of resonance state because similar states have been shown to exist in Cu adatom structures on Cu(111).[8] In the latter case the resonance state is formed in the prominent sp band gap of the Cu(111) surface.

B. Simple model for resonance states and images

To gain a better understanding of the interactions among the resonance states and the LDOS images for finite chains, we have analyzed our results in a simple tight binding, resonance (TBR) model with an s-wave approximation for the tails of the resonance wave functions in the vacuum region. This model is defined in the Appendix. The TBR model explains the success of and justifies the "particle-in-the-box" analysis of the observed scanning tunnelling spectra for the Au chains.

We begin by investigating to what extent the TBR model can describe the calculated resonance energies of the various
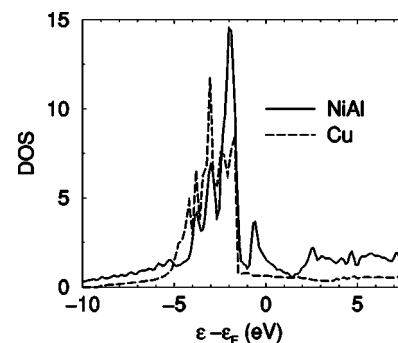
FIG. 9. Calculated bulk density of states of NiAl(110) (solid line) and Cu (dashed line).

adatom structures. One obvious choice of tight-binding parameters is based on the calculated energies of the resonance doublet of the ad-dimers. In the case of the ad-dimer Y, these energies are 1.2 and 2.1 eV, which are reproduced by an on-site energy $\epsilon_0 = 1.65$ eV and a nearest-neighboring off-site energy $t_1 = -0.45$ eV. Note that in this model ϵ_0 corresponds to the resonance energy for a single adatom and ϵ_0 is very close to the calculated value of 1.7 eV for the adatom. The predicted values for the resonance energies for the resonance triplet of the ad-trimer are then $\epsilon_0 + t_1/\sqrt{2} = 1.01$, $\epsilon_0 = 1.65$, and $\epsilon_0 - t_1/\sqrt{2} = 2.29$ eV. These values are in good agreement with the calculated energies for the two lowest-lying states but for the highest-lying state the calculated energy is too high with about 0.3 eV. In the case of the ad-dimer X, the resonance energies suggests on-site resonance energy, $\epsilon_0 = 1.70$ eV that is close to its value for the ad-dimer Y, whereas the off-site energy $t_1 = -0.30$ eV is smaller than its value for the ad-dimer Y.

In our earlier study of the resonance doublets in ad-dimers with various interatomic distances, we argued that there are both direct and substrate-mediated contributions to the adatom-adatom resonance interaction described by t_1. The origin of these contributions is clarified by the result of the TBR model for t_1 in Eq. (A6): $t_1 = t_1^D + t_1^S$ has a direct contribution t_1^D and a substrate-mediated contribution t_1^S. $t_1^D = Z t_1^{(0)}$ is given by the direct interaction between the $6s$ atomic orbitals being renormalized by their resonance strength Z. $t_1^{(0)}$ decays exponentially with the interatomic distance d whereas t_1^S is long ranged and was found to dominate t_1 for larger d. t_1^S can also have a negative imaginary part which would enhance and diminish the broadening for the symmetric and antisymmetric resonance states, respectively. However, this effect is not discernable in the calculated LDOS for the ad-dimers.

In the case of the infinite ad-chains, the sets of TB parameters derived from the ad-dimers give a poor description of the dispersions of the resonance states for the Y and X ad-chains. The predicted energies $\epsilon_0 + 2t_1 = 0.75$ and 1.10 eV of the lowest energy state of the TB model for the Y and X ad-chains, respectively, are in agreement with the calculated energies of 0.69 and 1.23 eV for the corresponding ad-chains. However, these parameters gives the wrong trend for the effective masses m^* for the ad-chains, as defined by the near-parabolic behavior of the dispersion for small wave vectors. The TB model with these parameters gives $m^* = \hbar^2/(2a^2 t_1) = 1.0$ and 0.75 m_e for the ad-chain Y and X, respectively, whereas from the calculated dispersion one obtains the reverse trend: $m^* = 0.65$ and 0.91 m_e for the ad-chain X and Y, respectively. Here a is the interatomic distance of the ad-chain. The breakdown of this model in describing both ad-dimers and ad-chains is a consequence of substrate-mediated long-range interactions among the resonance states, as was demonstrated by the combined theoretical and experimental study in Ref. 16 for the resonance states of ad-dimers with various interatomic distances. However, as shown in Fig. 4, the near-parabolic dispersion of the resonance states for wave vectors up to one-half of the LBZ is described well by the effective TB parameters $\epsilon_0 = 2.09$ (1.83) and $t_1 = -0.7$ (−0.25) eV for the Y (X) ad-chain. Note that for larger wave vectors, the strengths of the reso-
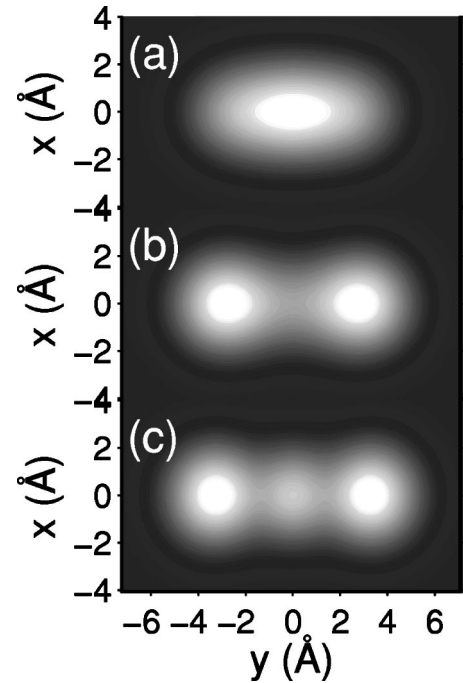
FIG. 10. Calculated local density of states images of a Au trimer on NiAl(110) within the tight-binding, resonance model. First, second, and third state at (a) 1.01, (b) 1.65, and (c) 2.29 eV, respectively. Same tip-surface distance as in Fig. 2.

nance states weakens and they become ill-defined.

We have also modelled the LDOS images using the TBR model augmented with an s-wave approximation for the vacuum tails of the wave functions from each resonance state (see the Appendix). In Fig. 10, we show the TBR-LDOS images of the three resonance states for the ad-trimer. The calculated images of the two first resonance states in Fig. 2 are rather well reproduced by this model. Note that the second state in the TBR model is antisymmetric and its amplitudes on the atoms are strictly localized to the edge atoms. The absence of a strict nodal plane in the corresponding image is caused by the resonance broadening so there is still a contribution from the first resonance state at the energy of the second resonance state. At the resonance energy of the third state, the TBR-LDOS image gives a too large contribution from the center adatom compared to the calculated LDOS image indicating that the resonance amplitude on the center adatom is relatively smaller to an edge adatom than in the TBR model. Note that the LDOS images do not directly reflect the resonance amplitudes on each adatom. For instance, in the TBR model the only difference between the resonance amplitudes on the adatoms between the first and the third resonance state is the sign of the amplitude of the center adatom and its magnitude is twice that for an edge adatom. The large suppression of the contribution of the center adatom to the TBR-LDOS image at the energy of the third resonance compared to that of the edge adatom is then caused by the destructive interference amongst the contribution from the center adatom to the LDOS and those from the edge atoms in contrast to a constructive interference of the contributions to the LDOS at the energy of the first resonance state.
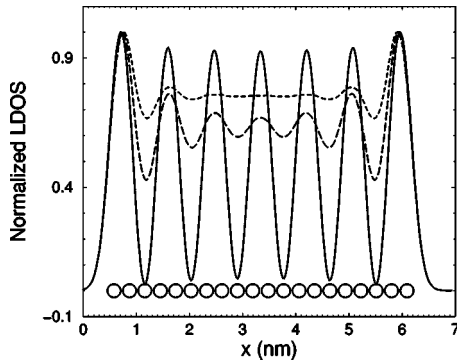
FIG. 11. Calculated profiles of model local density of states profiles of a 20 Au atom chain on NiAl(110) along Y within the tight-binding resonance model. The profile is along the ad-chain with the same tip-surface distance as in Fig. 1. First, second, and third profile is at an energy of 1.39 eV corresponding to the $n=7$ resonance state with a broadening γ equal to (a) 0.0, (b) 0.20, and (c) 0.40 eV, respectively. The circles indicate the positions of the atoms in the ad-chain.

FIG. 12. Energy variation of the lowest energy state in the ad-chain along the Y direction as a function of number of adatoms. The solid line is the result from the tight-binding, resonance model using the effective tight binding parameters obtained from the calculated dispersion, whereas the dashed line is the result using the "particle-in-the box" model with parameters obtained from the tight-binding resonance model. The solid diamonds are the experimental values taken from Refs. 3–5 and 7.

For the low-energy states of longer chains with relative long wavelengths compared to the tip-surface distance, the resonance broadening results in an enhancement of the LDOS at the edge atoms. This effect is illustrated in Fig. 11 by the results for the TBR-LDOS profiles at an energy corresponding to the seventh ($n=7$) resonance state of a chain with 20 atoms for three different values of the resonance broadening γ. At the lowest value of γ essentially only the $n=7$ state contributes to the LDOS and there is only a minor enhancement of the LDOS at the edge atom whereas the number of contributing states increases with γ and the enhancement increases at the edge atoms. At the largest value of γ, the nodal planes are no longer discernable. Alternatively, this effect may be understood simply as a reduction of the phase coherence length of an electron propagating along the chain by the resonance broadening.

V. COMPARISON WITH EXPERIMENTS

The unoccupied, resonance states of chains of Au atoms of various lengths on a NiAl(110) surface were characterized by a scanning tunnelling microscope both in an imaging and spectroscopy mode by Nilius and co-workers.[4,5] Here we are making a comparison of the calculated resonance energies for the ad-chain Y with their experimental data. In addition, the "particle-in-a-box" model used in the experimental analysis is clarified and justified by making a direct connection to the tight-binding resonance (TBR) model.

The calculated dispersion of the resonance states for the infinite, ad-chain along the Y direction is in agreement with the measured dispersion from the ad-chains with 11 (Au$_{11}$) and 20 (Au$_{20}$) adatoms. The dispersion for the Au$_{20}$ ad-chain was obtained from an analysis of the characters and the energies of the observed resonance states in the PIB model. For the Au$_{11}$ ad-chain the second, third, and fourth resonance state dominated the oscillations in the dI/dV spectra at 1.3–1.4, 1.7, and 2.5 V from which the number of nodal planes

and corresponding wavelengths of these states and the box length could be determined. A fit to a free-particle dispersion gave an effective mass of $0.4\pm0.1m_e$. For the Au$_{20}$ ad-chain, several resonance states contributed to the dI/dV spectra and the resonance energies, wavelengths and box length were extracted from a fit of the observed STS profiles to a superposition of several neighboring eigenstate densities of the particle in the box. The resulting effective mass of $0.5m_e$ is in close agreement with the result from the Au$_{11}$ ad-chain. The calculated value of $0.65m_e$ compares favorably with these measured values for the effective mass.

Another more direct observation of the electronic resonance state energies of the chain was the measurement of the energy, $\epsilon_{\min}(N)$, of the low-energy peak in the STS spectra as a function of the number of atoms N in the ad-chain. $\epsilon_{\min}(N)$ was found to follow closely the L^{-2} dependence obtained in the PIB model where L is the box length. Note that the relation between L and N is not well defined in the PIB model. The best fit was obtained using a weakly bias dependent L, which were in good agreement with chain lengths determined from STM topographic images. The calculated value of 0.69 eV for $\epsilon_{\min}(\infty)$ is very close to the band onset of 0.68 eV obtained from an extrapolation of the measured values to $N\rightarrow\infty$. For finite ad-chains, we can make a comparison of the calculated data with measured $\epsilon_{\min}(N)$ by using the result from the TBR model for

$$\epsilon_{\min}(N) = \epsilon_{\min}(\infty) - 4t_1 \sin^2\left(\frac{\pi}{2(N+1)}\right). \tag{3}$$

As shown in Fig. 12, the agreement of the results from this model using the effective TB parameters for the infinite, ad-chain is in excellent agreement with the experimental data. Note that the difference between the results of the TBR and the free-particle limit is not significant.

This good agreement between theory and experiment for the Au chains is somewhat fortuitous and is not granted by the use of unoccupied Kohn-Sham states. For example, in the

case of the resonance states of the adatom, the ad-dimers, and the ad-trimer the energy difference between calculated and measured resonance energies is typically up to 0.3 eV as shown in Fig. 1. As discussed in Ref. 3, a large part of this energy difference for the resonance in the single adatom can be accounted for by the Stark shift introduced by the electric field of the sample bias. However, in the case of the ad-trimer, the Stark shifts on the resonance energies are found to be small, that is, 0.014 to 0.03 eV for an external field of about 0.1 V/Å.

The success of the PIB model in the analysis of the observed dI/dV spectra and profiles, and some of its conceptual problems are clarified by the TBR model. For example, in the PIB model the physical meaning of the one-dimensional box and wave functions are not clear. For wave vectors well within the LBZ boundaries, the TBR model gives a free-particle-like dispersion of the PIB model. As shown in the Appendix, the envelopes of the resonance state amplitudes on the adatoms in the TBR model are the same as the wave function in the PIB model with $L=(N+1)a$. Furthermore, as shown in Fig. 11, the profile of the LDOS of a single, low-energy resonance state along the Au_{20} ad-chain in the TBR model is close to the density of the corresponding state in the PIB model. Note that for resonance states with higher energies and shorter wavelengths, the LDOS densities are enhanced at the endpoints.

VI. CONCLUDING REMARKS

We have carried out a density functional study of the unoccupied, resonance states in linear Au atom structures on a NiAl(110) surface. The primary objective has been to understand the character and the origin of these states, which were revealed and studied by scanning tunnelling microscopy and spectroscopy. The prime focus of this study has been infinite, chains of Au atoms along the two different orientations, [001] and [1$\bar{1}$0], on the NiAl(110) surface. The substantial difference in interatomic distances between these two different orientations of the ad-chains illustrates the effects of interatomic interactions. From a study of the evolution of the resonance states in an ad-chain from the states of the isolated chain, we find that the resonance states derives from the $6s$ states of the Au adatoms, which hybridize strongly with the substrate states and develop a substantial p-like polarization perpendicular to the surface.

The calculated resonance states and their local density of states images were analyzed in a tight-binding, resonance model. This analysis provides physical insight about these states. The origin behind and the distinction between direct and substrate-mediated interactions between the resonance states are clarified in the TBR model. The LDOS at the end atoms of finite ad-chains is shown to be enhanced by two different physical mechanisms. Finally, the physical meaning of "particle-in-box" model used in the analysis of STS for Au ad-chains is revealed in the TBR model.

The calculated effective mass of free-particle-like dispersion of resonance states for the infinite, Au ad-chain along the [001] direction is in good agreement with the measured effective mass, as obtained from STS of resonance states in

the ad-chain with 11 and 20 Au atoms. The calculated energy of the band bottom is in good agreement with the measured energy as obtained from an extrapolation of the measured energies of finite ad-chains to an infinite ad-chain length. The principal limitations of describing the unoccupied resonance states in the Au adatom structures by unoccupied Kohn-Sham states are revealed by the energy differences of about 0.1–0.3 eV between calculated and measured resonance energies for the ad-dimer and the ad-trimer.

APPENDIX

The proposed tight-binding resonance model of the resonance states in the linear adatom structures is based on a multisite Newns-Anderson (NA) model.[21,22] The Hamiltonian for this model is given by

$$H = \sum_i \epsilon_0^{(0)} \hat{c}_i^\dagger \hat{c}_i + \sum_{i,j} (t_{ij}^{(0)} \hat{c}_i^\dagger \hat{c}_j + \text{h.c.}) + \sum_i \sum_\mu (V_{i\mu} \hat{c}_i^\dagger \hat{c}_\mu + \text{h.c.})$$
$$+ \sum_\mu \epsilon_\mu \hat{c}_\mu^\dagger \hat{c}_\mu \qquad (A1)$$

Here $\hat{c}_i^\dagger$ creates an electron in an adatom state at site i of the adatom structure with energy $\epsilon_0^{(0)}$ and $t_{ij}^{(0)}$ is the direct interaction (hopping) term between two adatoms at site i and j, $V_{\mu i}=V_{i\mu}^*$ is the interaction (hopping) term between an adatom state at site i and a substrate state μ with energy ϵ_μ and an electron in this state is created by $\hat{c}_\mu^\dagger$. Note other atomic states can be included among the substrate states. The result for the adatom Green function for a single site[22] generalizes directly to the multisite model as,

$$G_{ij}(\epsilon) = (G_i(\epsilon)^{-1} \delta_{ij} - t_{ij}^{(0)} - \Sigma_{ij}(\epsilon)(1-\delta_{ij}))^{-1}, \qquad (A2)$$

where the Green function, $G_i(\epsilon)$, for a single adatom at site i is given by

$$G_i(\epsilon) = ((\epsilon - \epsilon_0^{(0)}) - \Sigma_{ii}(\epsilon))^{-1}. \qquad (A3)$$

The effect of the substrate is represented by an energy-dependent and complex self-energy as

$$\Sigma_{ij}(\epsilon) = \sum_\mu \frac{V_{i\mu} V_{\mu j}}{\epsilon - \epsilon_\mu + i0^+}. \qquad (A4)$$

The resonance of the single Au adatom on the NiAl(110) surface at the site i is now modelled as a simple pole at $\epsilon_0 - i\gamma$ in the $G_i(\epsilon)$ for the $6s$ state with a pole strength Z. Note that in this case the magnitude of Z will be substantially less than unity. Now we assume that for energies around $\epsilon_0+i\gamma$

the energy dependence of the off-diagonal part of $\Sigma_{ij}(\epsilon)$ can be neglected so that

$$G_{ij}(\epsilon) \approx Z((\epsilon - \epsilon_0 + i\gamma)\delta_{ij} - t_{ij})^{-1}, \qquad \text{(A5)}$$

where t_{ij} is a renormalized hopping term given by

$$t_{ij} = Z(t_{ij}^{(0)} + \Sigma_{ij}(\epsilon_0)). \qquad \text{(A6)}$$

This hopping term has a contribution $Zt_{ij}^{(0)}$ from the direct interaction between $6s$ atomic states renormalized by the resonance strength and a contribution $Z\Sigma_{ij}(\epsilon_0)$ from substrate-mediated interactions. Here, we restrict t_{ij} to nearest-neighbor interactions. Using these approximations, the multisite adatom Green function reduces to an analytic form given by

$$G_{ij}(\epsilon) = Z\sum_k \frac{\psi_{ki}^* \psi_{ki}}{\epsilon - \epsilon_k + i\gamma_k}, \qquad \text{(A7)}$$

where the energies ϵ_k and the amplitudes ψ_{ki} are the same as in the nearest neighboring TB model for a chain of states and are given by

$$\epsilon_k = \epsilon_0 + 2\,\text{Re}(t_1)\cos(ka), \qquad \text{(A8)}$$

$$\psi_{ki} \propto \sin(k|\vec{x}_i|), \qquad \text{(A9)}$$

where t_1 is the nearest neighboring hopping term and $\vec{x}_i$ are the positions of the N adatoms in the linear ad-chain with nearest neighboring adatom-adatom distance a, and k $= n\pi/(N+1)a, n=1,2,\ldots,N$. In contrast to the standard TB model, t_1 can have a negative imaginary part from the substrate-mediated interactions resulting in a k-dependent broadening γ_k given by

$$\gamma_k = \gamma - 2\,\text{Im}(t_1)\cos(ka). \qquad \text{(A10)}$$

Finally, note that $\text{Im}(t_1) < 0$ will tend to increase the broadening with decreasing k and that this model contains the ad-dimer and the ad-trimer as special cases, corresponding to $N=2$ and 3, respectively.

Using this TBR model, we have also generated a model LDOS at the tip apex $\vec{r}_0$ and an energy ϵ by a superposition of localized wave functions as

$$\rho(\vec{r}_0; \epsilon) = \sum_k \left| \sum_i \psi_{ki}\phi(\vec{r} - \vec{x}_i; \epsilon) \right|^2 \frac{1}{\pi((\epsilon - \epsilon_k)^2 + \gamma^2)}. \qquad \text{(A11)}$$

Here we have neglected any k-dependent broadening. At the tip apex, we use an s-wave approximation for the vacuum tail of $\phi(\vec{r}; \epsilon)$ given by

$$\phi(\vec{r}; \epsilon) \propto \exp(-\kappa r)/r, \qquad \text{(A12)}$$

where κ is the decay of the wave function in the vacuum.

*Electronic address: tfymp@fy.chalmers.se

[1] M. F. Crommie, C. P. Lutz, and D. M. Eigler, Science **262**, 218 (1993).

[2] E. J. Heller, M. F. Crommie, C. P. Lutz, and D. M. Eigler, Nature (London) **369**, 464 (1994).

[3] N. Nilius, T. M. Wallis, M. Persson, and W. Ho, Phys. Rev. Lett. **90**, 196103 (2003).

[4] T. M. Wallis, N. Nilius, and W. Ho, Phys. Rev. Lett. **89**, 236802 (2002).

[5] N. Nilius, T. M. Wallis, and W. Ho, Science **297**, 1853 (2002).

[6] N. Nilius, T. M. Wallis, and W. Ho, Phys. Rev. Lett. **90**, 186102 (2003).

[7] G. V. Nazin, X. H. Qiu, and W. Ho, Science **302**, 77 (2003).

[8] S. Fölsch, P. Hyldgaard, R. Koch, and K. H. Ploog, Phys. Rev. Lett. **92**, 056803 (2004).

[9] A. Görling, Phys. Rev. A **59**, 3359 (1999).

[10] G. Mills, B. Wang, W. Ho, and H. Metiu, J. Chem. Phys. **120**, 7738 (2004).

[11] K. H. Hansen, J. Gottschalck, L. Petersen, B. Hammer, E. Laegs- gaard, F. Besenbacher, and I. Stensgaard, Phys. Rev. B **63**, 115421 (2001).

[12] G. Kresse and J. Hafner, Phys. Rev. B **47**, 558 (1993).

[13] G. Kresse and J. Furthmüller, Phys. Rev. B **54**, 11 169 (1996).

[14] G. Kresse and D. Joubert, Phys. Rev. B **59**, 1758 (1999).

[15] J. P. Perdew, J. A. Chevary, S. H. Vosko, K. A. Jackson, M. R. Pederson, D. J. Singh, and C. Fiolhais, Phys. Rev. B **46**, 6671 (1992).

[16] B. Hammer, L. B. Hansen, and J. K. Norskov, Phys. Rev. B **59**, 7413 (1999).

[17] P. Feibelmann, B. Hammer, J. K. Nørskov, F. Wagner, M. Scheffler, R. Stumpf, and J. Dumesic, J. Phys. Chem. B **105**, 4018 (2001).

[18] J. Tersoff and D. R. Hamann, Phys. Rev. Lett. **50**, 1998 (1983).

[19] N. D. Lang, Phys. Rev. B **34**, 5947 (1986).

[20] H. L. Davis and J. R. Noonan, Phys. Rev. Lett. **54**, 566 (1985).

[21] P. W. Anderson, Phys. Rev. **124**, 41 (1961).

[22] D. M. Newns, Phys. Rev. **178**, 1123 (1969).